C. R. Physique 17 (2016) 389–405

Contents lists available at ScienceDirect

Comptes Rendus Physique

www.sciencedirect.com

Condensed matter physics in the 21st century: The legacy of Jacques Friedel

Structure of covalently bonded materials: From the Peierls distortion to Phase-Change Materials

Structure des matériaux covalents : de la distorsion de Peierls aux matériaux à changement de phase

Jean-Pierre Gaspard [a,b,*]

[a] *University of Liège, B5, B-4000 Sart-Tilman, Belgium*
[b] *Institut Laue-Langevin, 71, avenue des Martyrs, 38000 Grenoble, France*

ARTICLE INFO

Article history:
Available online 28 December 2015

Keywords:
Covalency
Peierls distortion
Symmetry breaking
Thermal expansion
Phase-change materials

Mots-clés :
Covalence
Distorsion de Peierls
Brisure de symétrie
Expansion thermique
Matériaux à changement de phase

ABSTRACT

The relation between electronic structure and cohesion of materials has been a permanent quest of Jacques Friedel and his school. He developed simple models that are of great value as guidelines in conjunction with *ab initio* calculations. His local approach of bonding has both the advantages of a large field of applications including non-crystalline materials and a common language with chemists. Along this line, we review some fascinating behaviors of covalent materials, most of them showing a Peierls (symmetry breaking) instability mechanism, even in liquid and amorphous materials. We analyze the effect of external parameters such as pressure and temperature. In some temperature ranges, the Peierls distortion disappears and a negative thermal expansion is observed. In addition, the Peierls distortion plays a central role in Phase-Change Materials, which are very promising non-volatile memories.

RÉSUMÉ

La relation entre structure électronique et cohésion des matériaux a été un sujet d'étude permanent de Jacques Friedel et de son école. Il a développé des modèles simples, intuitifs qui se sont révélés des guides d'une grande valeur et par la suite un complément utile aux calculs ab initio.

Son approche locale de la liaison chimique s'applique à un vaste champ de systèmes, incluant les matériaux non cristallins et permis un langage commun avec les chimistes. Dans cet axe nous passons en revue quelques comportements fascinants des matériaux covalents, la plupart d'entre eux présentant un mécanisme d'instabilité de Peierls (brisure de symétrie), même les liquides et les amorphes, étonnamment. Nous analysons aussi l'effet de parame'tres externes tels que la pression et la température. Dans un certain domaine de température, la distorsion de Peierls disparaît et une dilatation thermique négative est observée. Enfin, la distorsion de Peierls joue un rôle central dans les matériaux

* Corresponding author at: University of Liège, B5, B-4000 Sart-Tilman, Belgium.
E-mail address: jp.gaspard@ulg.ac.be.

http://dx.doi.org/10.1016/j.crhy.2015.12.009

à changement de phase (PC materials), qui sont très prometteurs pour la réalisation de mémoires non volatiles.

1. Covalent materials: structure–cohesion–electronic properties

Covalent materials have shown a constantly renewed interest in the last seventy years, mainly because of their electronic properties. Jacques Friedel and his school studied extensively the relation between structure, electronic structure and cohesion of covalent materials using simple, elegant models of the cohesion. A semi-empirical quantum mechanical model (with a limited number of parameters) has the advantage of being applicable to a large series of structures, crystalline and non-crystalline, liquid, surfaces, clusters.... The tight-binding approximation of independent electrons has proven very successful and applicable to a large variety of situations. Following a very first application on the band structure of semiconductors [1], the model has been generalized to amorphous semiconductors [2,3]. Extensive applications have been made in the field of semiconductor surfaces and defects [4]. The octet rule $Z = 8 - N_{\rm sp}$, where Z is the coordination number and $N_{\rm sp}$ is the number of s and p electrons in the valence shell was demonstrated along these lines [5].

We shall mainly focus on elements of columns V, VI and VII of the periodic table. They are covalent materials, and their crystal structure may be viewed as a distorted, simple cubic one (Fig. 1). We will show that this originates from their electronic structure and the directionality of the p-orbitals. The distortion arises from a symmetry-breaking mechanism related to the Peierls distortion.

The Peierls distortion (PD) is an instability of one-dimensional metals. It is explained by J.-P. Pouget in the present issue [6,7] and in [8]. The mechanism is summarized in Fig. 2 below.

The periodicity of the Peierls distortion depends on the filling of the band or the number of electrons per atom e/a as illustrated in Fig. 1. The role of e/a on the crystallographic structure has been considered previously by Hume-Rothery as emphasized by Jacques Friedel. The Peierls distortion has been first described in his lectures notes (Les Houches, 1953, see inset in Fig. 2) and later in a textbook [9].[1] However, the idea of a symmetry breaking mechanism in group V elements (Bi) has been considered by H. Jones [10] as early as 1934 and discussed in the celebrated book of Mott and Jones [11].

In this paper, we extend the concept of Peierls distortion to three-dimensional systems, we derive its condition of occurrence and its importance when it is present or vanishes.

2. Minimal model of distortion

The two ingredients of the chemical bond or cohesion, namely electromagnetism and quantum mechanics, are well established, but due to the fact that many electrons and nuclei are interacting, the problem has no exact analytic solution. Consequently, there are different theories of cohesion and various levels of approximation. In a minimal model, the covalent bond can be simply described by a sum of two energies: an attractive part due to the resonance of the valence orbitals (s and p in covalent materials), described by a resonance integral $\beta(r)$ and a pairwise additive repulsive potential $V_{\rm rep}(r)$. Both are decreasing functions of the distance and are expressed by a power law [12] or an exponential function.[2]

$$\begin{aligned} \beta(r) &= \frac{\beta_0}{r^q} \\ V_{\rm rep}(r) &= \frac{V_0}{r^p} \end{aligned} \tag{1}$$

with $p > q$. The attractive (electronic) part originates from the band broadening by resonance. Typical values of the q parameter are between 2 and 3 for covalent materials [12]. Let us stress the importance of the repulsive term in the structure of materials [13], especially when a distortion appears. The repulsive term is usually neglected in the chemical literature and the experimental equilibrium distance is taken [14]. It is difficult to model the repulsive energy as it originates not only from the electrostatic repulsion but also from Pauli's exclusion principle. The hardness of the repulsion is characterized by the exponent p.

Let us start with a very simple model that contains all the ingredients of the symmetry-breaking mechanism and that shows under which conditions the highest symmetry (or highest coordinated) structure is the most stable. In 1D, 2D or 3D in a system with Z neighbors, with isotropic interactions, the second moment (variance) of the electronic density of states $n(E)$ is $Z\beta^2$, hence the bandwidth is proportional to $\sqrt{Z}\beta$ (second moment approximation [15]). This is a consequence of the quantum mechanical character of the covalent bond. With a pairwise additive repulsive term the total energy writes, per atom:

[1] But he never published it in a research paper.

[2] The relevant parameter is the dimensionless logarithmic derivative of the function, β or V, at the equilibrium separation.

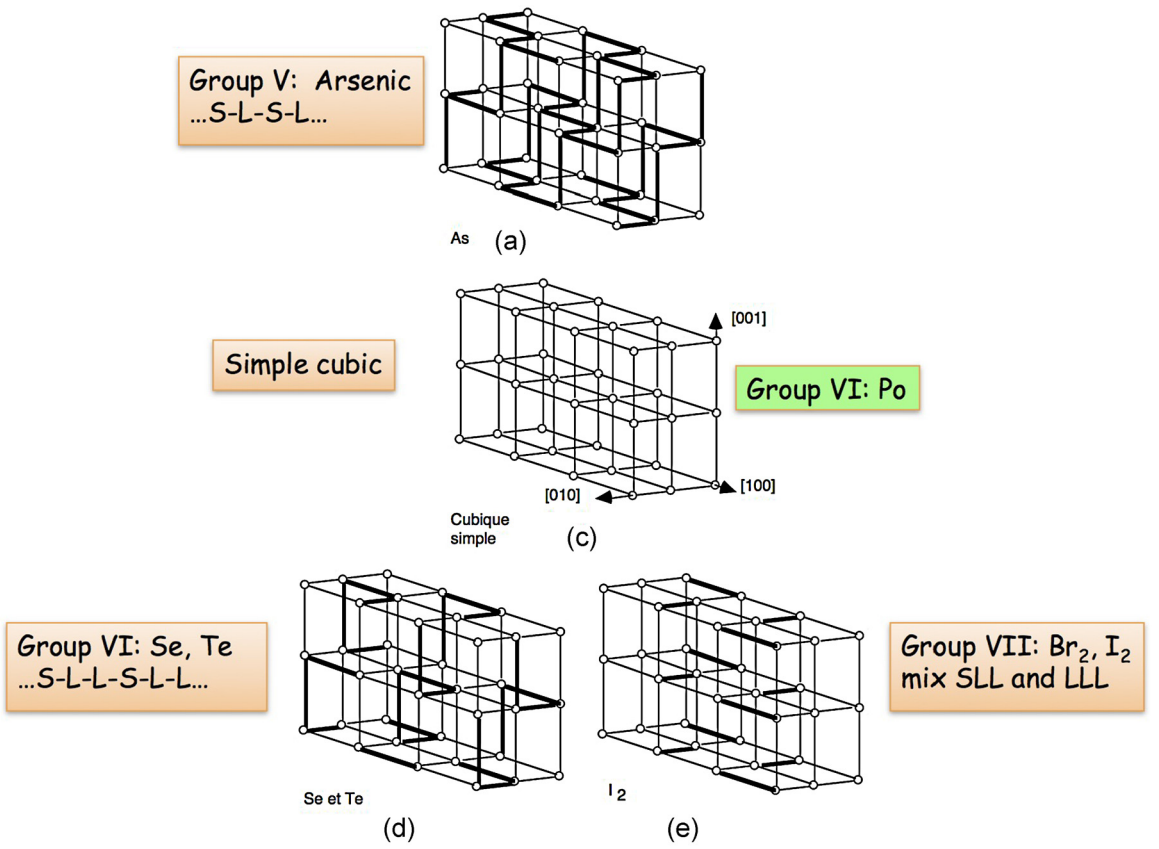

Fig. 1. A large number of group V, VII and VII structures can be related to a deformation (symmetry breaking) of a simple cubic structure. Polonium is the exception. The short covalent bonds are in bold and the long Van der Waals bonds are in light. The coordination numbers of groups V, VI and VII are respectively 3(+3), 2(+4) and 1(+5).

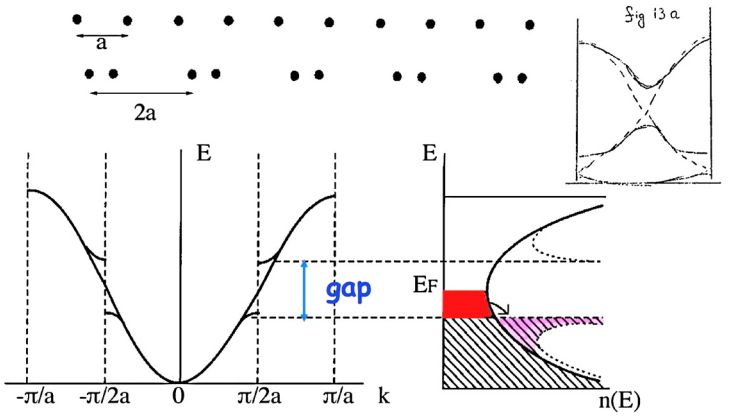

Fig. 2. Dispersion relation $E(k)$ and density of states of undistorted and distorted chain. The energy gain is the consequence of the downwards shift (arrow) of the occupied energy levels close to the Fermi energy (in red). Upper right insert: original drawing in Peierls' Les Houches lecture notes.

$$E_{\text{coh}} = \frac{Z}{2}\frac{V_0}{r^p} - \sqrt{Z}\frac{\beta_0}{r^q} \tag{2}$$

As a consequence, the equilibrium distance is an increasing function of Z: the more neighbors, the larger the interatomic separation, indeed the minimum of (2) gives

$$r_{\text{eq}} = \left(\frac{pV_0}{2q\beta_0}\right)^{\frac{1}{p-q}} Z^{\frac{1}{2(p-q)}} \tag{3}$$

and the cohesive energy E_{coh} at the equilibrium distance r_{eq} varies as

$$E_{\rm coh}^{\rm eq} \propto Z^{\frac{p-2q}{2(p-q)}} \tag{4}$$

The sign of the exponent in (4) depends on the hardness of the repulsion.

In a system with a hard repulsion ($p > 2q$) the higher the coordination number, the more cohesive the structure; this is, e.g., the case of the transition metals. At the opposite, with a soft repulsion ($p < 2q$) the system distorts and the maximum of cohesion (in absolute value) corresponds to the smallest coordination number ($Z = 2$). Consequently, for soft isotropic potentials, the structure is made of diatomic molecules. This is the case of hydrogen H_2. Let us stress that the result (4) originates from the difference in Z-dependence of the two terms in (2). If both terms were proportional to Z, $E_{\rm coh}^{\rm eq}$ would also be proportional to Z (pairwise additive) and the maximum coordination would be favored (as, e.g., in rare gases).

Let us remark that this elementary model does not even include symmetry considerations; the sole parameter is the coordination number Z.

For a more accurate treatment, one should now take the directionality of the orbitals. The situation is different in the different columns of the periodic table. In columns I and II, only s-orbitals are populated, which have spherical symmetry and no directionality is involved. The corresponding elements are metals with a compact structure (FCC, BCC, ...). A similar situation occurs in column III where the s electrons dominate (s^2p electronic configuration). For the right-hand side of the periodic table, p-orbitals are partly occupied, and may hybridize with s orbitals. Using a simple model similar to the formula (2), but including the orbital directionality, one finds [12] that elements of columns V, VI and VII have no sp hybridization, so that the s-band is full and only p-orbitals are relevant for chemical binding. On the contrary, the elements of column IV show a hybridization of s- and p-electrons. The remainder of this paper is focused on columns, V, VI and VII.

2.1. Group V, VI and VII elements

The covalent elements of column V, VI and VII are bonded through the p electrons that show a strong directionality with their 3 perpendicular lobes of the $3p_x$, p_y and p_z orbitals. This suggests that a simple cubic structure (SC) (Fig. 1, center) is a good starting approximation. Indeed, it maximizes the overlap between p-orbitals, therefore the resonance energy β, the bandwidth, and the cohesive energy. Since the p-band is partially occupied, the simple cubic structure is a metallic state. But this structure is unstable and distorts into a semiconducting or an insulating structure. The distortion is very similar to the Peierls distortion. Indeed if one considers for instance Fig. 1a, and a chain of atoms parallel to the [100] axis, the p_x electrons of this chain are weakly coupled to the p_x electrons of the parallel chains. If the other two orthogonal p-orbitals are neglected, a Peierls distortion is therefore expected for that chain as well as for all chains parallel to the [100] axis. The effect of the other two p-orbitals is obviously to distort chains parallel to the [010] and [001] axes. It turns out that the distortion corresponds to a dimerization, as shown in Fig. 1a. Other combinations of the distortions of different chains may lead to different structures.

Let us first consider the simplest case of group V elements in the A7 structure, in which two distances, short $r_{\rm S}$ and long $r_{\rm L}$, alternate (Figs. 1 and 2 and Table 1). Appropriate variables are

$$\bar{r} = \frac{1}{2}(r_{\rm S} + r_{\rm L})$$
$$\eta = \frac{r_{\rm L} - r_{\rm S}}{r_{\rm S} + r_{\rm L}} \quad -1 \leqslant \eta \leqslant 1 \tag{5}$$

η measures the strength of the Peierls distortion, $\eta = 0$ corresponds to a periodic linear chain in 1D or a simple cubic structure in 3D. For a given value of $\bar{r}$, the energy E can be expanded in power series of η. In a strictly one-dimensional conductor, there is a term proportional to $\eta^2 \ln \eta$ as shown by Peierls [16]. However, in the systems of interest here, an analytic expansion is expected, namely

$$E = E_0 + A\eta^2 + B\eta^4 + \ldots \tag{6}$$

The coefficient A of the quadratic term determines whether a distortion occurs ($A < 0$) or not ($A > 0$) and the quartic term defines its position and amplitude. The softer the repulsive potential, the stronger the distortion. A more precise model may be introduced, based on the second moment of the density of states [10, 12]. The energy takes the form, in one dimension

$$E = \frac{V_0}{2}\left(\frac{1}{r_{\rm S}^p} + \frac{1}{r_{\rm L}^p}\right) - \beta_0 f(N_e)\sqrt{\frac{1}{r_{\rm S}^{2q}} + \frac{1}{r_{\rm L}^{2q}}} \tag{7}$$

where β_0 is a constant and $f(N_{\rm e})$ is a function of the number of electrons $N_{\rm e}$ (related to $E_{\rm F}$), which depends weakly on the shape of the density of states. The most used models of the density of states are the two-level (bonding and anti-bonding) model, the constant (rectangular) density of states (the so-called Friedel model) and a Gaussian density of states. In, any case, the function $f(N_{\rm e})$ shows a maximum when the band is half-filled as all the bonding states are occupied and the anti-bonding states are empty. Despite its relative simplicity, formula (7) accounts for many properties of covalent systems and it generates rich behaviors. Different energy landscapes are shown in Fig. 3.

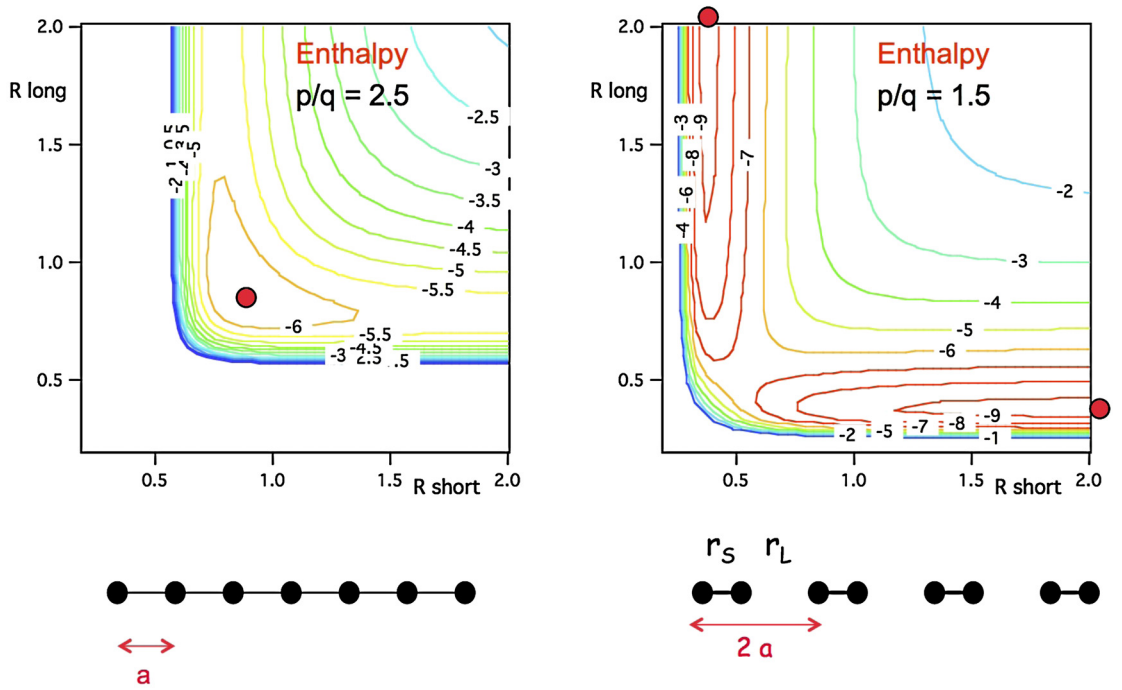

Fig. 3. Energy landscape corresponding to Eq. (7). Peierls non-distorted (left) and distorted (right). The red point corresponds to the energy minimum.

A series expansion of (7) around the equilibrium distance $\bar{r}$ of the undistorted structure, gives to fourth order in η:

$$E = -\frac{\beta_0}{\bar{r}^q}\left[(1-\frac{q}{p}) + \frac{q}{2}(p-2q)\eta^2 + \gamma\eta^4\right] \tag{8}$$

γ is a polynomial in p, q. If $p > 2q$ the energy minimum occurs on the diagonal of the plane (r_S, r_L) (Fig. 3, left). When $p < 2q$ two minima occur in symmetric positions. The crude tight binding model at zero pressure predicts a distortion with infinite long bonds ($r_L = \infty$) (Fig. 3, right). The addition of Van der Waals interactions (or an external pressure) gives finite long bonds. The successive curves of Fig. 5, from bottom to top, from violet to black correspond to going down in the periodic table. The distortion becomes weaker and weaker as the repulsive coefficient p increases. Polonium is the only element showing a simple cubic structure; it corresponds to the black curve. Alternatively the curves correspond to decreasing volumes (or increasing pressures) from bottom to top. The value of η at the minimum and the relative energy gain ΔE_P of the Peierls distortion are given, for $p < 2q$, by $\eta = \sqrt{\frac{q(2q-p)}{4\gamma}}$ and $\Delta E_L/E_{band} = -\frac{q^2(p-2q)^2}{16\gamma}$.

2.2. Resonant bonding

The so-called **resonant bonding**, a term coined by L. Pauling, corresponds to the case of a weak Peierls distortion with two shallow minima (green curve in Fig. 5). The anharmonicity becomes severe. In the marginal case of a vanishing η^2 term in (8) the restoring force for the η coordinate is very weak as the linear term vanishes (red curve); the force is in η^3. The vibration ellipsoid is extremely elongated along a direction at 45° to the axis (Fig. 4). As a result, a soft mode appears and a pronounced electron delocalization occurs and gives rise to an increased electronic polarizability that is observed experimentally [20]. This is of primary relevance in two issues discussed in the next sections: negative thermal expansion and phase change materials.

For the group V, VI and VII elements, the s electrons do not play an important role in the bonding process, unlike the group IV elements. Using a simple model similar to Eq. (2), but including orbital directionality [12], one demonstrates that the limit between tetrahedral coordination (sp^3 bonding) and octahedral coordination (p bonding) is given by the number of electrons N^*_{sp}

$$N^*_{sp} \simeq 5. - \frac{\varepsilon_p - \varepsilon_s}{2|\beta_{sp^3}|} \tag{9}$$

where ε_s and ε_p are respectively the valence s and p energy levels and β_{sp^3} the resonance integral between two sp^3 hybrid orbitals pointing towards one another. The higher the hybridization energy $\varepsilon_p - \varepsilon_s$, the lower N^*_{sp}.

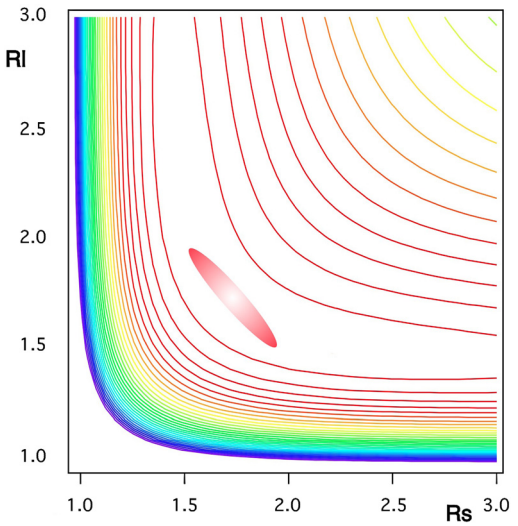

Fig. 4. Energy landscape in the case of the resonant bonding. The vibration ellipsoid is very elongated along a direction at 45°.

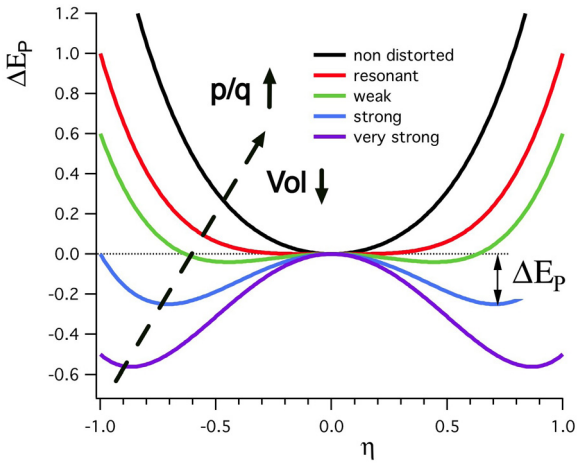

Fig. 5. Energy as a function of the distortion parameter η (schematic). The reference energy is the energy of the undistorted structure. The different curves can be seen in different ways: (1) as a function of the element in a periodic table, (2) as a function of the volume (or pressure), (3) as a function of the ratio p/q.

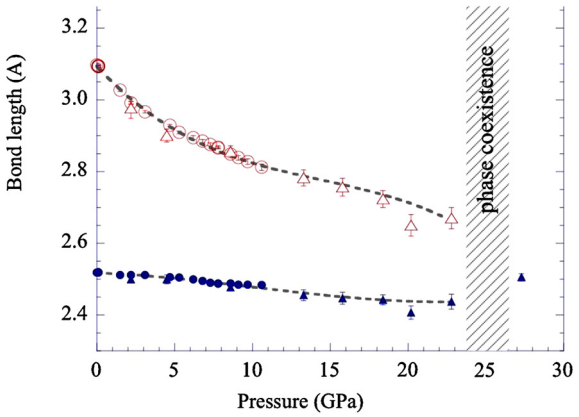

Fig. 6. Short and long distances of the A7 structure of arsenic measured by EXAFS.

Table 1
Parameters of group V and VI elements and GeTe (from [14]). The value of the ratio p/q increases when going down the periodic table. The ratio of the Peierls energy to $k_B T_m$ fixes the persistence or not of the Peierls distortion in the liquid. Z_l is the average coordination number of the liquid [17–19].

Element	r_C	r_L/r_C	η	p/q	T_m (K)	$\Delta E_P/k_B T_m$	Z_l
P	2.19	1.77	.28	3.8	873	–	–
As	2.51	1.25	.11	4.9	1090	1.5	3.5
Sb	2.87	1.17	.08	5.3	904	.75	6.3
Bi	3.10	1.12	.06	5.5	544	.2	6.8
Se	2.32	1.49	.20	5.5	494	.2	2.1
Te	2.86	1.31	.13	5.5	723	.2	3.0
Po	3.36	1.00	.00	5.5	527	.2	–
GeTe	2.83	1.11	.05	5.7	100	.1	4.5

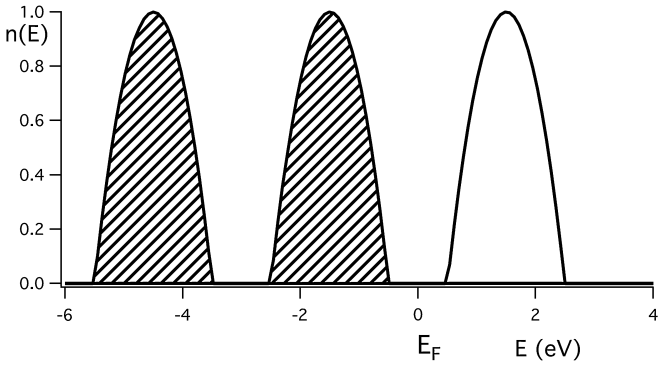

Fig. 7. Schematic density of state of state of the Se or Te structure $(SLL)_n$. From left to right: bonding band, lone pair band and unoccupied anti-bonding band.

In the case of an alloy, the same formula holds for the average number $\bar{N}^*_{sp}$ of s and p electrons, at least in the case of heavy elements (see Table 3).

As β_{sp^3} and $\varepsilon_p - \varepsilon_s$ are rather close (e.g., for Si), N^*_{sp} is about 4.5 in good agreement with the facts that Si is tetrahedrally coordinated and As is hexacoordinated (with an additional Peierls distortion).

2.3. Band filling and the octet rule

As previously said, the periodicity of the Peierls distortion depends on the filling of the band (Fig. 1); the number of electrons per atom plays a central role.

For the elements of column V with a 1/2-filled p band, the doubling of the periodicity $(SLSLSL\ldots = (SL)_n)$[3] stabilizes the structure (Fig. 1 (top) and Fig. 2).

For the elements of column VI, with a 2/3 filled p band, every third bond is strong and short, and each atom is strongly linked to two atoms (instead of three for column V) and weakly linked to four atoms (Fig. 1 (d)). A trebling of the periodicity $(SLLSLL\ldots = (SLL)_n)$ occurs, usually called a trimerization.

Finally the atoms of column VII associate as diatomic molecules (Br_2, I_2, etc.) as expected $(1 + (5)$ coordination).

The Peierls distortion opens a band gap at the Fermi energy E_F with the consequence that the highest occupied energy levels[4] are pushed down with a gain of electronic energy (provided that the repulsive term does not compensate this energy gain).

For the elements of column VI, a gap opens at E_F, with an additional gap at 1/3 filling without any energy effect (Fig. 7) for the latter.

In general, for a m/n filling of the band,[5] one obtains a n-periodic structure, i.e. the periodicity of the original linear chain is multiplied by n and $n-1$ band gaps appear, but only the gap close to E_F has a stabilizing action. This is observed in many elements and compounds, in particular in binary and ternary compounds of group V and group VI elements. Systematic crystallographic studies have shown that the rule is fulfilled by a large series of compounds (see Table 2) [21–23,14].

Tellurium deserves a special attention. Under normal conditions of temperature and pressure, tellurium follows the octet rule, it is 2-coordinated (Te^{II}) but it may adopt a coordination 3 (Te^{III}) under other circumstances: in the liquid phase as suggested by B. Cabane and J. Friedel [24], or when it is alloyed with an element with a fewer number of electrons (e.g., GeTe). This may be understood schematically from the electronic configuration. Indeed in Fig. 8, one sees that Te^{II} and Te^{III}

[3] S = short, L = long.
[4] In chemical parlance, the HOMO and states just below.
[5] m and n are relative prime numbers.

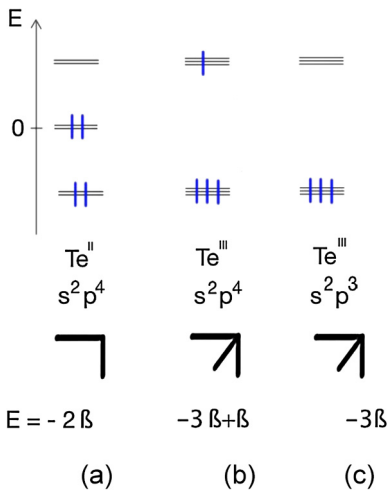

Fig. 8. Electronic energies of Te in different environments. Te^{II} (a) and Te^{III} (b) have the same electronic energy but if Te transfers an electron to Ge, the Te^{III} (c) configuration is more stable. β is the modulus of the resonance integral $pp\pi$.

Table 2
m-Merization of different elements and compounds with partly filled *p* bands [21,22]. The filling ratio of the p band is expressed by the ratio of two prime numbers m/n [23].

Compound	m/n	*n*-merization
P (black)	$1/2 = .500$	2
As, Sb, Bi	$1/2 = .500$	2
GeTe	$1/2 = .500$	2
Se, Te	$2/3 = .667$	3
β-As_2Te_3, Sb_2Te_3	$3/5 = .600$	5
Bi_2Se_3, Bi_2Te_3	$3/5 = .600$	5
$GeSb_2Te_4$	$4/7 = .571$	7
Sb_2Te	$5/9 = .556$	9
$Ge_2Sb_2Te_5$	$5/9 = .556$	9
$As_2Ge_3Te_6$	$6/11 = .545$	11
$As_2Ge_5Te_8$	$8/5 = .533$	15
Bi_4Se_9	$10/17 = .588$	17
$Bi_{14}Te_6$	$11/20 = .550$	20
$As_2Ge_8Te_{11}$	$11/21 = .524$	21
Bi_6Te_5	$19/33 = .576$	33
Bi_8Te_7	$26/45 = .576$	45
α-Po	$2/3 = .667$	1

have the same electronic energy. The repulsive energy favors the Te^{II} geometry [5] because it has only two repulsive energies instead of 3 for Te^{III}. But if an electron of Te (or a fraction of it) is transferred to Ge, the structure becomes more stable as the anti-bonding level is depleted. This explains the A7 structure of GeTe, in which the Te atoms are 3(+3) coordinated, which can be seen alternatively as a Peierls distortion of a NaCl structure.

In liquid Te, due to the local thermal fluctuations of the volume, the delicate energy balance of Te^{II} and Te^{III} (Fig. 8) justifies the coexistence of both species [24,25].

2.4. Individual or collective behavior

Up to now, we have considered "average" atoms with a corresponding average number of p electrons (Table 2). In a covalent alloy, does each atomic species behave with its proper number of electrons or do the atoms behave as if they had an average number of electrons? In other words, is the octet rule satisfied locally or in the average? Table 3 gives an experimentally answer to this question for the IV–VI compounds. If the octet rule is satisfied locally one has an AB_2 compound; if it is satisfied, in the average one has an AB stoichiometry. One observes that the lighter atoms have a stronger tendency to individualism (4-coordination for group IV atoms and 2-coordination for group VI atoms, e.g. SiO_2), while the heavier ones share their electrons more easily. In the latter, a rock-salt structure is obtained, mainly due to the directionality of the p orbitals with a subsequent Peierls distortion, finally Ge and Te atoms both have a coordination 3(+3). The octet rule is fulfilled for "average" atoms with 5sp electrons per atom and a coordination 3.

The relevant parameter that drives the relative stability of tetrahedral versus octahedral coordination is the metallicity parameter $\alpha_m = (\varepsilon_p - \varepsilon_s)/|\beta_{sp^3}|$, ratio of the promotion energy to the resonance (or band) energy. The lower this parameter

Table 3
Existing compounds of composition AB_2 or AB. The number below is the average of the period numbers $\overline{Pn}$ of the periodic table. A clear separation occurs for $\overline{Pn} = 4$.

atom		C	Si	Ge	Sn	Pb
	Pn	2	3	4	5	6
O		CO_2	SiO_2	GeO_2	SnO_2	PbO_2, PbO
$\overline{Pn}$	2	2	2.5	3	3.5	4
S		CS_2	SiS_2	GeS_2	SnS_2, SnS	PbS
$\overline{Pn}$	2.5	2.5	3	3.5	4	4.5
Se		CSe_2	$SiSe_2$	$GeSe_2$, GeSe	SnSe	PbSe
$\overline{Pn}$	3	3	3.5	4	4.5	5
Te		CTe_2	$SiTe_2$, SiTe	GeTe	SnTe	PbTe
$\overline{Pn}$	3.5	3.5	4	4.5	5	5.5

Table 4
Average values of the promotion energy $\varepsilon_p - \varepsilon_s$, resonance integrals β_{sp^3} and metallicity parameter α_m of SiO_2 and GeTe.

	SiO_2	GeTe
$\varepsilon_p - \varepsilon_s$ (eV)	11	9.3
d (Å)	1.61	3.0
β_{sp^3} (eV)	13	3.7
α_m	.85	2.5

(less cost for hybridization) the more favorable the octahedral structure. SiO_2 and GeTe have comparable hybridization energies $\varepsilon_p - \varepsilon_s$, but the value of $|\beta_{sp^3}|$ is larger for SiO_2 because of the shorter interatomic separation (Table 4).

2.4.1. Pressure effects

Pressure reduces the Peierls distortion as the weak long bonds shrink more than the short bonds under pressure. In an exact treatment in 1D, the Peierls distortion is still present at all pressures (or volumes) [26]. Experimentally, the distortion is suppressed above some transition pressure P_P and the simple cubic structure is restored. Interestingly enough, the approximate model (7) shows the same behavior. A typical example is arsenic ($P_P = 25$ GPa), as shown in Fig. 6. The transition is second order in the tight-binding approximation. Let us notice that, in close vicinity to the transition pressure P_P, the short bonds elongate because the coordination number increases but, of course, the total length (or volume in 3D) diminishes. The rhombohedral-to-cubic transition in GeTe has also been observed at room temperature under a hydrostatic pressure of 3.5 GPa [27]. This phase transition is found to be first order with a 3% volume change.

2.5. Peierls distortion in disordered systems

The original Peierls mechanism,[6] related to a translational symmetry in a 1D crystal, can be extended in different directions, even in non-crystalline systems. In summary, in the simplest case, the Peierls distortion is an alternation of short and long bonds $(SL)_n$. The doubling of the periodicity of the linear chain opens a gap at the Fermi energy E_F. The highest occupied states, those just below E_F, are displaced downwards giving rise to a gain of electronic energy [9]. The original demonstration of Peierls relied on the dispersion relations ($E(k)$, Fig. 2) but the mechanism is far more general. In systems without translational invariance, and no longer dispersion relations, we consider instead the density of electronic states $n(E)$. A lowering of the density of states at E_F also produces a gain of electronic (band) energy (Fig. 9). A "à la Peierls" distortion may be present in disordered systems. The electronic energy is the average energy of the occupied states $E_{el} = \int^{E_F} En(E)\,dE$, i.e. it increases (in absolute value) when an "erosion" occurs at E_F, which shifts down the highest occupied levels. A simple calculation shows that the energy gain is proportional to the surface of the displaced states. The simplest example of a Peierls distorted non-crystalline structure is liquid H_2.

In disordered systems (amorphous or liquid), the situation is less simple, but a strong analogy with symmetry breaking and dimerization exists, mainly because the chemical bond is local by nature. Let us note that Eqs. (4) and (7) do not assume that the system is crystalline, hence they are applicable to disordered systems. The structural analysis has to be treated in a statistical way using at least a three-body correlation function that can be analyzed by computer simulation. An analogous alternation can be detected in the following way: an atom (1) is selected in the structure, and one of its nearest neighbors (2) is picked at a distance r_1, then in a cone of small aperture (e.g., 30°, Fig. 10), we pick the closest atom (3) at a distance r_2. We then compute the distribution of the distances (r_1, r_2) for all the atoms at any time in the course of the simulation.

[6] For extended systems, the Peierls distortion is the analogous of the Jahn–Teller effect in finite systems (molecules, vacancies, ...).

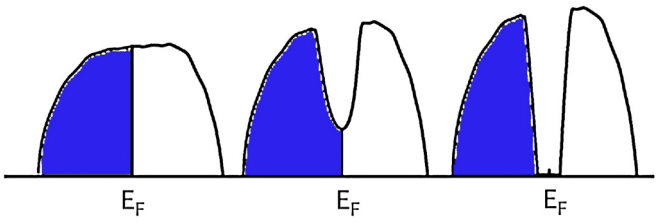

Fig. 9. Densities of states and Peierls distortion. Left: non-distorted. Middle: Peierls distorted in liquid with a dip at the Fermi level at E_F. Right: Peierls distortion of a crystal with a gap at E_F.

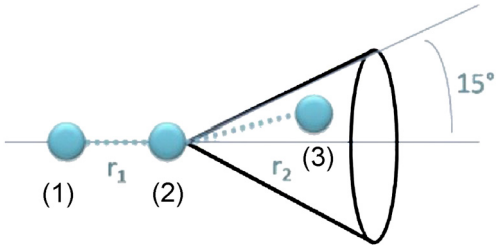

Fig. 10. Geometry of the three-body correlation function $p(r_1, r_2)$ for three almost aligned atoms.

Fig. 17 shows the probability density of the distances (r_1, r_2) for $Ge_{15}Te_{85}$ just above the melting point. The double-peak structure shows that there is clearly a three-body correlation: a short bond is followed by a long bond and vice-versa. The Peierls distortion is still present in average in the liquid. At higher temperature, the double peak is no longer visible and the Peierls distortion is removed. The following rule of thumb applies: if ΔU_P is smaller than $k_B T$, the Peierls distortion is still present but if ΔU_P is smaller than $k_B T$, the Peierls distortion disappears or is hardly visible.

Experimentally, the existence of a "à la Peierls" distortion in a liquid has been proved, e.g., in liquid arsenic by neutron scattering (Fig. 11) [28]. Liquid As has a low coordination number $Z_l \approx 3$–3.5 similar to the case of the A7 crystalline structure, which is made of parallel corrugated sheets of As atoms with a coordination $3(+3)$ with distances $r_S = 2.51$ Å and $r_L = 3.00$ Å. In the case of As, the Peierls energy ΔU_P is larger than the thermal energy $k_B T_m$ and consequently the Peierls distortion survives the melting (Table 2). This is no longer the case of heavier elements of column V (Sb, Bi). For the latter, above T_m, the distortion disappears and a coordination of ≈ 6 or larger is found.

In column VI, Se is Peierls distorted in the liquid with a coordination of ≈ 2, whilst Te has a higher coordination (3 and more, depending on the temperature) [24].

Still more interesting, in the case of a weak Peierls distortion, a multiple reentrant behavior may occur. This is the case of GeTe that, which shows a rich behavior. Above the α–β transition of GeTe, melting occurs at 998 K with volume expansion. This volume expansion favors the recurrence of the distortion, which finally disappears at very high temperature. In short, with increasing the temperature, we have the sequence PD (α-GeTe) $\Rightarrow$ NonPD (β-GeTe) $\Rightarrow$ PD (l-GeTe) $\Rightarrow$ NonPD (l-HT-GeTe), i.e. a doubly reentrant transition [29].

2.6. Group IV elements

Despite the fact that they also fulfill the octet rule, the bonding properties of group IV elements are a little more complex and they do not fall into the preceding simple picture as both s and p electrons come into play. In addition, the lightest atom, carbon, shows some departure with respect to the octet rule as it may adopt coordination 3 or 2 (with sp^2 or sp hybrids), giving rise to the extraordinary rich field of organic chemistry and important structures such as fullerenes, carbon nanotubes, and graphene, with very promising physics. On the contrary, silicon and germanium do not give rise to multiple bonds. The silicene structure with exciting potential applications has been hoped and searched extensively. However, silicon fullerenes as well as silicon nanotubes and silicene do not exist under ambient conditions. Epitaxial growth of graphene-like silicon nanoribbons has been reported [30]. Accommodated silicon adsorption layers on the (111) Ag surface have been observed instead of sp^2 silicene strips [30–32]. The difference between carbon and the heaviest column IV elements lies in their larger interatomic separations and ultimately in their repulsive potential. C has no closed shell if we except the $1s^2$ shell, whilst the heavier column IV elements have one or more closed shells that increase the hardness p of the repulsive potential.

In Fig. 12, the energies of different structures (diamond, graphite, linear chain) are plotted as a function of p, taking into account the directionality of the various hybrids [12]. One clearly sees that graphite is more stable than diamond only for very soft repulsive interactions. This explains why Si, Ge and Sn do not show graphene-like structures.

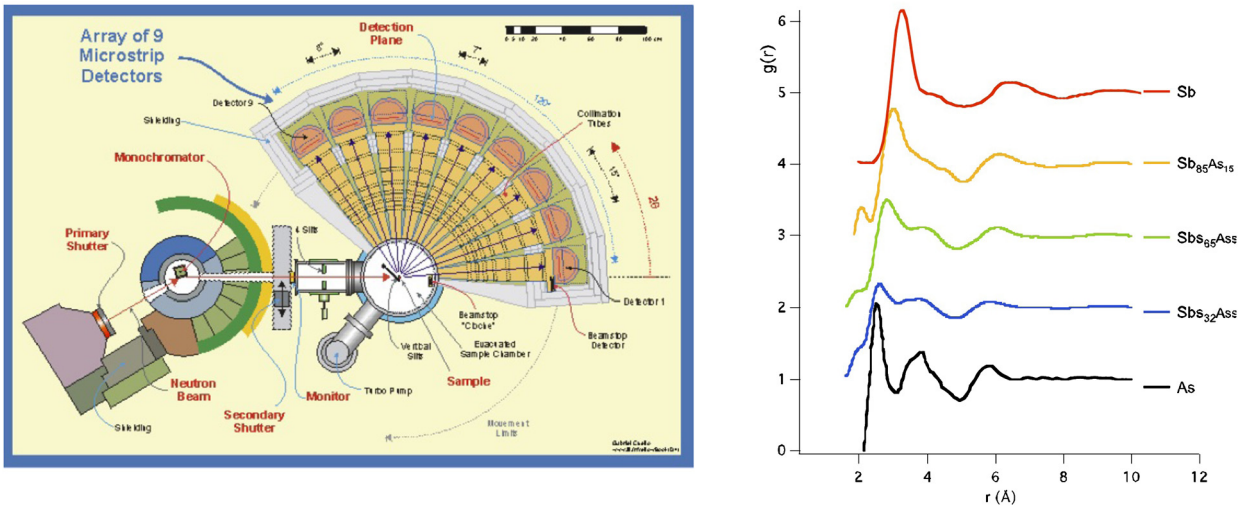

Fig. 11. (Left) Experimental setup (D4 diffractometer at ILL). (Right) Pair correlation functions of liquid alloys of As and Sb and coordination numbers. One observes a continuous disappearance of the Peierls distortion when Sb is added to As.

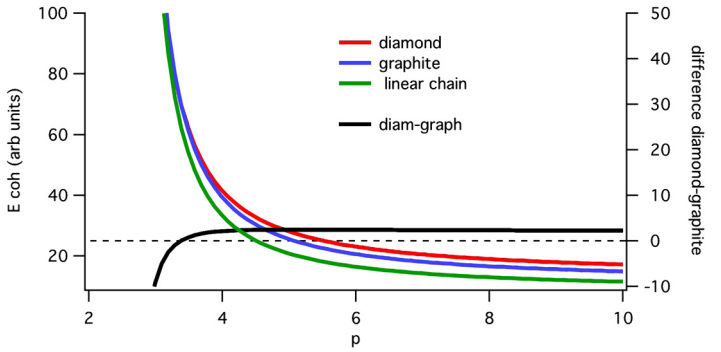

Fig. 12. Energies of diamond, graphite and polymeric chain as a function of the hardness p of the repulsive potential. Right scale: difference diamond–graphite. Graphite is the most stable structure for soft repulsive potentials $p < 3.3$, i.e. only for C.

3. Negative thermal expansion

Even if it is not very common, several materials show a negative thermal expansion (NTE). Different bonding mechanisms may produce this effect [33]. In covalent materials, the disappearance or the weakening of the Peierls distortion is the origin of the NTE.

α-GeTe is isoelectronic to As and shows also the rhombohedral A7 structure ($R\bar{3}m$) at room temperature, i.e. it is Peierls distorted with a coordination 3(+3) with two distances: 2.84 Å and 3.15 Å. At 705 K, the system undergoes a phase transition to β-GeTe, a NaCl structure with six distances of 2.98 Å up to the melting temperature $T_m = 998$ K[7] (Fig. 13). The rhombohedral-to-cubic phase transition in GeTe is accompanied by a volume contraction of 0.6% and its nature – displacive or not – is still under discussion [34]. This volume contraction is analogous to the NTE in liquids discussed hereafter.

Liquid Te expands when it melts, but in the supercooled regime, below $T_m = 723$ K, its thermal expansion is negative between 573 K and 723 K (Fig. 14) [35], with a 10% contraction and thermodynamic anomalies. The enthalpy increases steeply by 4 kJ/mole. Bernard Cabane and Jacques Friedel [24] suggested that Te, which is weakly Peierls distorted, has a local order in the liquid consisting of sites with two or three first neighbors, joined by bonds with a strong covalent character. The structural change in Te is characterized by a strongly peaked extremum in the specific heat c_P, isothermal compressibility and thermal expansion coefficient. If a lighter element (Ge, As or Se) is added to Te, the NTE domain lies, partly or totally, in the normal liquid phase, close to the melting temperature. Fig. 14 shows the severe decrease in the atomic volume of some Ge_xTe_{1-x} alloys in a temperature range of more than 150 K. The NTE is related to the disappearance of the Peierls distortion when temperature increases. By neutron scattering, a characteristic prepeak is observed in the structure factor $S(q)$ at ≈ 1 Å^{-1} (Fig. 15), which is the signature of the Peierls distortion corresponding to a periodicity of

[7] The melting temperature may vary with some departure from the stoichiometry. Different values are found in the literature.

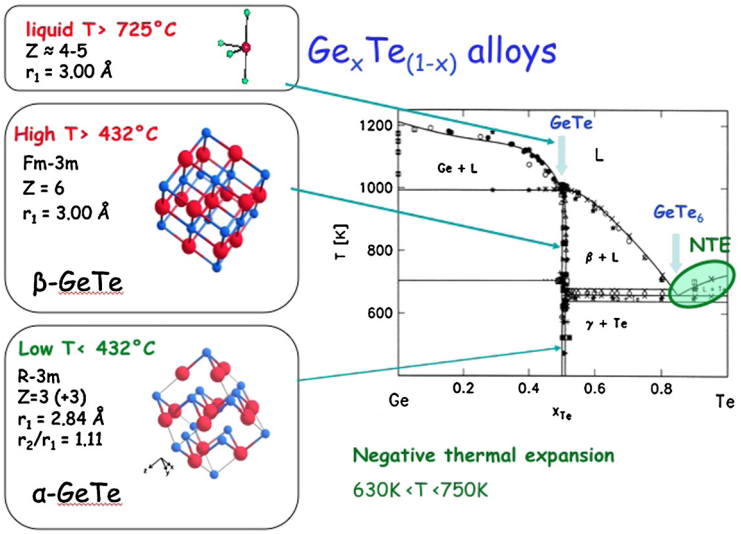

Fig. 13. Phase diagram of the alloy Ge_xTe_{1-x} and crystallographic structures of the compound GeTe. In green, the region of negative thermal expansion (NTE).

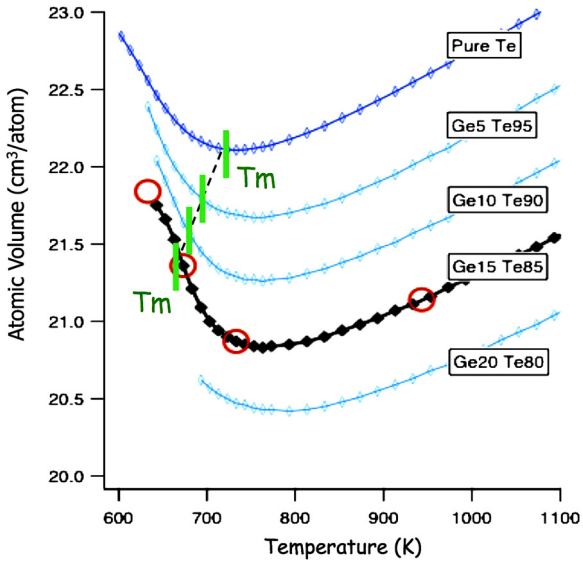

Fig. 14. Temperature evolution of the atomic volume of liquid alloys Ge_xTe_{1-x}.

$\cong 6$ Å; this corresponds to an alternation of short and long bonds similarly to l-As. This alternation disappears gradually with temperature.

Computer simulations shed some light on the mechanism of the NTE. In Fig. 16, the case of liquid As_2Te_3 is illustrated. The curves give the average distances of the 1st, 2nd, … nearest neighbors (not in the common sense) of an atom. More precisely, for each atom, the successive distances to its successive neighbors (the closest, the next, …) are computed and their distributions are calculated and time averaged. The maxima of the partial distributions are shown in Fig. 16. At low temperature, the octet rule is fulfilled (three short and three long distances) for As, and for Te (two short and four long distances), while at higher temperatures the distribution of distances is continuous and the Peierls distortion is no longer visible. As the long distances decrease more than the short distances increase, a shrinking of the volume follows. Hence the relation between the disappearance of the Peierls distortion and the NTE. This can be rationalized on the basis of the two-well model (Fig. 5).

The mechanism of the NTE in covalent materials is explained the following way (Fig. 18). At some temperature T, the system vibrates along the η coordinate with an amplitude σ that gives rise to a vibrational entropy S. If $k_BT \lesssim \Delta E_P$, i.e. just below the dotted line, the structure shrinks. Indeed, in the balance $F = E - TS$, the system reduces its volume with an energetic cost, but with an entropic gain that overcompensates the energetic penalty. As the short distances increase, the vibrational modes soften, as it has been demonstrated by inelastic neutron scattering [36,37]. The upper panels of Fig. 17

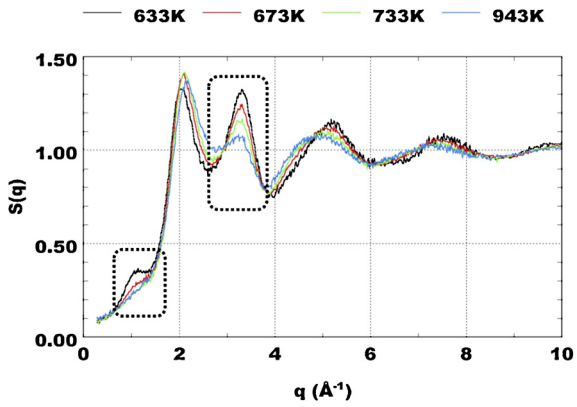

Fig. 15. Structure factor of $Ge_{15}Te_{85}$. The prepeak at ~ 1 Å^{-1} is the signature of a Peierls distortion in the liquid. It diminishes gradually when the temperature increases as well as the second main peak.

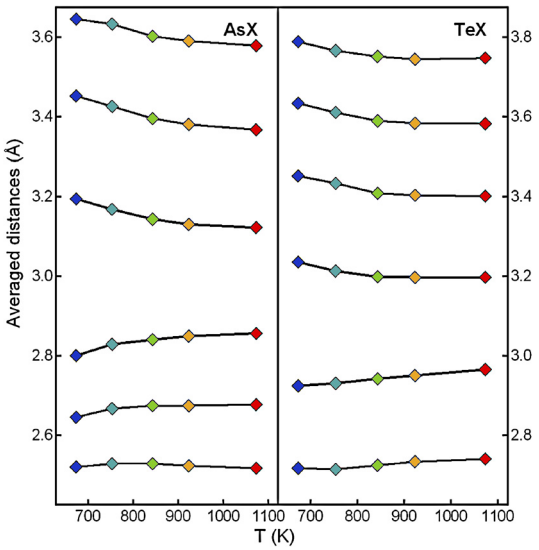

Fig. 16. Distances of the successive nearest-neighbor average distances as a function of the temperature of liquid As_2Te_3.

summarize the result: just above the melting temperature, the system is distorted; in this case a Ge atom is off-centered in the cage of Te atoms, while at higher temperature, the cage is smaller and the Ge atom is centered at least in the average.

In summary, the NTE is a transition from a Peierls distorted state to a weakly distorted state (or a resonant bonding state).

We conjecture that this NTE effect should occur in any covalent material in some (P, T) domain, solid or liquid, but it appears in the vicinity of the melting temperature only in a few systems. It is the case of a series of Te-based compounds.

4. Phase-Change Materials

Among the many applications of covalent compounds, the Phase-Change Materials (PCM) for data storage devices are important and challenging. They are based on the fast reversible switching between an amorphous and a crystalline state with a contrast in their optical and electronic properties enabling data storage. Rewritable digital versatile (DVDs) and Blu-ray disks and non-volatile RAMs are based on covalent alloys. Most of them are tellurium-based compounds (Fig. 20). Using a laser or an electrical current, a small part (a few 100 nm^3) of the crystal is heated above the melting temperature T_m. The extremely high cooling rate ($\approx 10^{10}$ K/s) prevents the liquid from crystallization and a melt-quenched amorphous bit is produced. The recrystallization is performed by annealing the amorphous bit above the glass transition temperature T_g, but below the melting temperature T_m (Fig. 19). As suggested by S. Ovshinsky in the late 1960s [38], the contrast in the optical and electrical properties of the two phases qualifies them as materials for data storage.[8]

[8] But the expected electronic revolution awaited four decades.

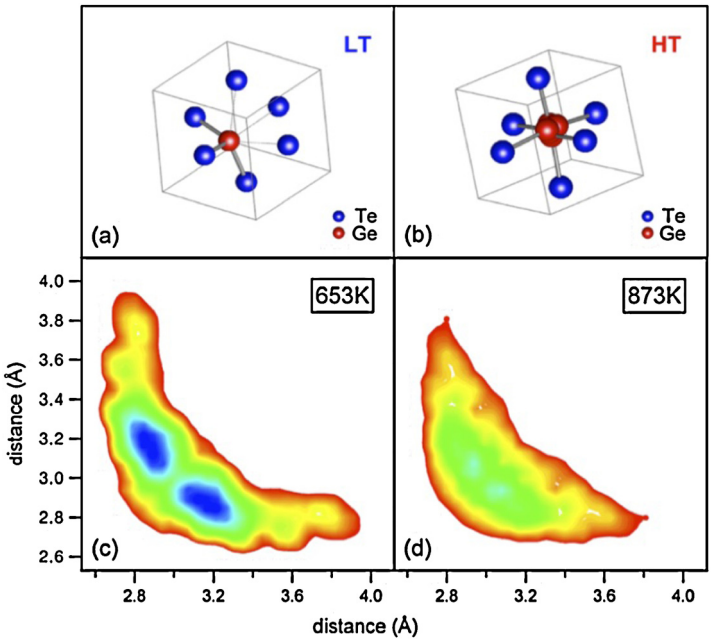

Fig. 17. Upper panel: low- and high-temperature structures of $Ge_{15}Te_{85}$. Lower panel: probability densities of two distances (r_1, r_2).

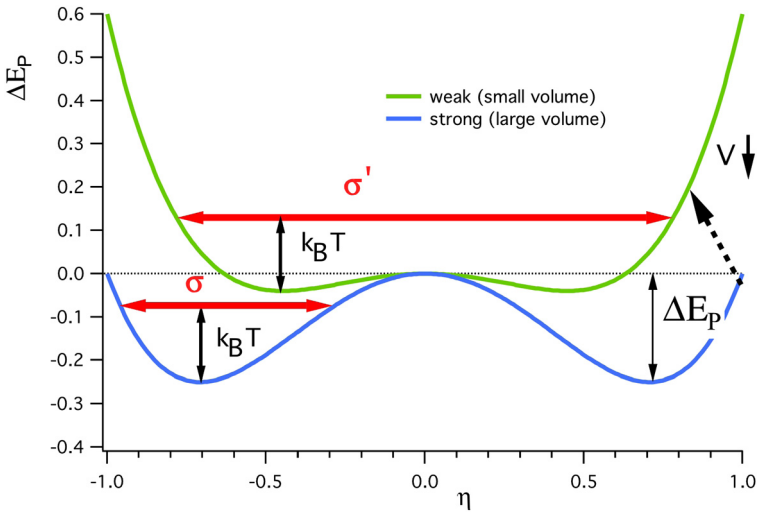

Fig. 18. Blue curve: vibrational amplitude (in red) at the temperature $k_B T$, just below the Peierls energy ΔE_P. A reduction of the volume at the same temperature transforms the blue curve into the green curve, for which the vibrational amplitude and entropy are higher.

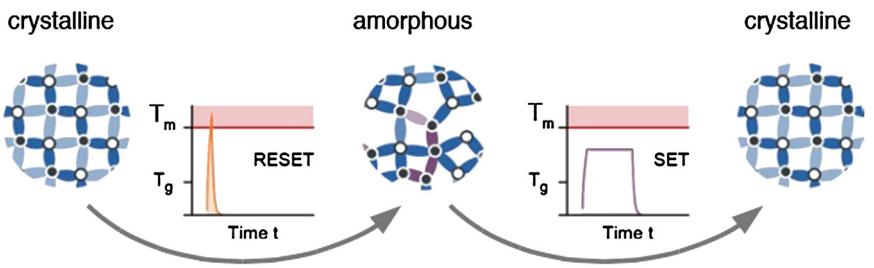

Fig. 19. The operation principle of a PCM device is based on the reversible switching between a crystalline and an amorphous phase that show a contrast in their optical and electrical properties [39].

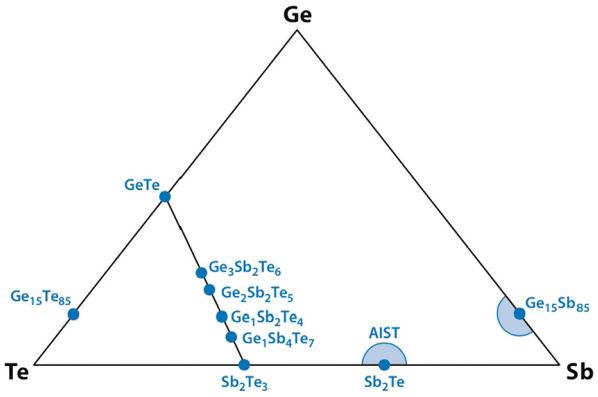

Fig. 20. Ternary phase diagram of GeSbTe. Tie line of Phase-Change Materials and eutectic composition $Ge_{15}Te_{85}$.

These Te-based alloys crystallize in a metastable NaCl structure, where Te atoms occupy one lattice site and Ge and Sb atoms and vacancies occupy the second lattice site.

The simplest PCM is GeTe, but for practical applications $Ge_2Sb_2Te_5$ is the model composition. The second sublattice is occupied by two Ge and two Sb atoms and one vacancy per unit cell, hence the (225) composition. In the amorphous structure, homopolar bonds may appear [40] and favor the occurrence of Ge atoms in tetrahedral coordination (Ge^{IV}). There are intense debates on the existence and role of tetrahedral Ge atoms (Ge^{IV}) [39] and many studies have been published both experimentally (EXAFS, diffraction, electron microscopy, ...) and by computer simulations.

The two structures – amorphous and crystalline – differ from their density and the amplitude of the Peierls distortion; these differences are at the origin of the contrast. Astonishingly enough, the crystal is less Peierls distorted than the amorphous structure. This can be understood, to a first approximation, by the higher density of the crystal, despite its 10% vacancies.

The crystal structures of phase-change materials are all based on distorted cubic structures and all possess resonant bonding that is the cause of the large optical dielectric constant observed in many crystalline IV–VI compounds [20], larger than in pair-bonded materials because it gives a smaller average band-gap and larger optical matrix elements as shown by Littlewood [41,42]. In the contour map of Fig. 4, the isochore oscillations are large and give rise to a large polarizability.

Aging is an important issue as the material is expected to perform a high number of cycles. Reference [40] develops smart techniques to simulate the relaxation of a melt-quenched amorphous structure of GeTe, to circumvent the fact that the *ab initio* molecular dynamic computer simulations cannot simulate directly timescales of – say – seconds. The relaxation "expels" the fourfold coordinated Ge atoms. The final relaxed amorphous structures are locally similar to the A7 crystalline structure with a 3(+3) coordination, but with a larger Peierls distortion; the lower density of the amorphous structure explain this at least in part. Indeed, the amorphous phase is inhomogeneous and, in addition, by aging, nano-segregation may occur. Fig. 21 compares GeTe in the liquid, amorphous and crystalline states, with the same density (for the sake of comparison), the density of the amorphous phase. The liquid is less distorted than the two solid phases due its the thermal disorder, but if the liquid were at its true density, it would have been still more distorted. One sees that the two principal axes of the symmetric vibration ellipsoids are nearly aligned in the case of the crystal – this is the signature of the resonant bonding –, whereas in the case of the amorphous phase, the principal axes cross at a finite angle. This should be reinforced if the crystal were at its true density, slightly higher than the amorphous phase. The amorphous phase is more distorted than the crystalline one because of its lower density.

From the point of view of Te, instead of being two-coordinated in pure Te, it is three-coordinated in the alloy as explained in Fig. 8 and Ref. [5]; indeed, if we neglect the repulsive energy, twofold coordinated Te^{II} and threefold coordinated Te^{III} have the same electronic energy. If we assume a partial charge transfer to the Ge atom, the Te^{III} gets more stable than the Te^{II}. Alloying a Te atom with an electron acceptor stabilizes the Te^{III} local configuration.

Finally, like in normal chalcogenide glasses, the local relaxed amorphous structure of phase change materials resembles that of the crystal, qualitatively but differs qualitatively and this produces the contrast. In terms of the simple model (eq. (7)), the candidates to PCM are the systems for which $p \simeq 2q$. Then, one of the structures, presumably the crystalline one, is close to the resonant bonding. Due to the larger Peierls distortion of the amorphous structure, the electronic gap is larger, hence the contrast.

5. Conclusion: universality of the Peierls distortion

We conjecture that all covalent materials involving column V, VI and VII elements undergo a Peierls distortion in some (P, T) domain. This is evidenced by their low coordination numbers.

As a consequence, all these covalent systems should show a negative thermal expansion at some temperature T_{NTE} related to the energy of the Peierls distortion ΔE_P. Roughly the central temperature T_{NTE} is simply given by

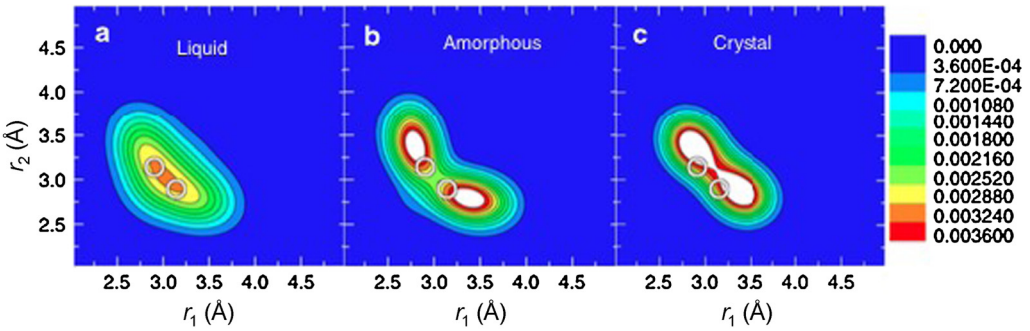

Fig. 21. Bond length distribution around a Ge atom in crystalline, liquid and relaxed amorphous GeTe. The panels represent the probability density $f(r_1, r_2)$ of having a bond of length r_1 almost aligned with a bond of length r_2 (angular deviations smaller than 25°). (a) liquid phase at $T = 1100$ K, (b) relaxed glass obtained by substituting Sn with Ge in a-SnTe and (c) crystal. All three systems are calculated at the same density: the density of the amorphous phase. The white open circles correspond to the maxima (r_1, r_2) in crystalline GeTe at the crystalline density. The plots show that the Peierls distortion amplitude $(r_2/r_1$ or η (5)) in relaxed amorphous GeTe is larger than in the crystalline phase (figure adapted from [40]).

$$T_{\mathrm{NTE}} = \frac{\Delta E_{\mathrm{P}}}{k_{\mathrm{B}}} \tag{10}$$

The simple models of cohesion, developed along the ideas of Jacques Friedel's school, allow us to understand the physics of these systems and are used as guides in tailoring materials.

References

[1] G. Leman, J. Friedel, J. Appl. Phys. 33 (1962) 281–285.
[2] J. Friedel, M. Lannoo, J. Phys. (Paris) 34 (1973) 115–121.
[3] J. Friedel, M. Lannoo, J. Phys. (Paris) 34 (1973) 483–493.
[4] M. Lannoo, J. Bourgoin, Point Defects in Semiconductors in Theoretical Aspects, Springer Series in Solid-State Sciences, vol. 22, 1981.
[5] J.-P. Gaspard, A. Pellegatti, F. Marinelli, C. Bichara, Philos. Mag. B 77 (1998) 727–744, http://dx.doi.org/10.1080/13642819808214831.
[6] J.-P. Pouget, C. R. Physique 17 (3–4) (2016) 332–356, in this issue.
[7] J. Villain, M. Lavagna, P. Bruno, C. R. Physique 17 (3–4) (2016) 276–290, in this issue.
[8] R. Hoffmann, Rev. Mod. Phys. 60 (1988) 601–628, http://dx.doi.org/10.1103/RevModPhys.60.601.
[9] R.E. Peierls, Quantum Theory of Solids, Oxford Classic Texts in the Physical Sciences, vol. 23, Oxford University Press, Oxford, UK, 1955.
[10] H. Jones, Proc. R. Soc. Lond., Ser. A, Mat. 147 (1934) 396–417.
[11] N.F. Mott, H. Jones, The Theory of the Properties of Metals and Alloys, Clarendon Press, 1936.
[12] W.A. Harrison, Electronic Structure and the Properties of Solids: The Physics of the Chemical Bond, Courier Corporation, 2012.
[13] F. Ducastelle, in: Interatomic Potential and Structural Stability, Springer, 1993, pp. 133–142.
[14] J.K. Burdett, Chemical Bonding in Solids, Oxford University Press, 1995.
[15] F. Cyrot-Lackmann, Adv. Phys. 16 (1967) 393–400.
[16] R.E. Peierls, More Surprises in Theoretical Physics, Princeton Series in Physics, vol. 19, Princeton University Press, Princeton, NJ, USA, 1991.
[17] J.-P. Gaspard, R. Bellissent, A. Menelle, C. Bergman, R. Ceolin, Nuovo Cimento D 12 (1990) 649–655.
[18] M. Mayo, E. Yahel, Y. Greenberg, G. Makov, J. Phys. Condens. Matter 25 (2013) 505102.
[19] J. Akola, N. Atodiresei, J. Kalikka, J. Larrucea, R. Jones, J. Chem. Phys. 141 (2014) 194503.
[20] K. Shportko, S. Kremers, M. Woda, D. Lencer, J. Robertson, M. Wuttig, Nat. Mater. 7 (2008) 653–658, http://dx.doi.org/10.1038/nmat2226, http://www.nature.com/nmat/journal/v7/n8/suppinfo/nmat2226_S1.html.
[21] R. Imamov, S. Semiletov, Sov. Phys. Crystallogr. 15 (1971) 845–850.
[22] H.W. Shu, S. Jaulmes, J. Flahaut, J. Solid State Chem. 74 (1988) 277–286.
[23] J.-P. Gaspard, R. Ceolin, Solid State Commun. 84 (1992) 839–842, http://dx.doi.org/10.1016/0038-1098(92)90102-F, http://www.sciencedirect.com/science/article/pii/003810989290102F.
[24] B. Cabane, J. Friedel, J. Phys. (Paris) 32 (1971) 73.
[25] C. Bichara, J.-Y. Raty, J.-P. Gaspard, Phys. Rev. B 53 (1996) 206.
[26] D. Khomskii, Basic Aspects of the Quantum Theory of Solids: Order and Elementary Excitations, Cambridge University Press, 2010.
[27] L. Khvostantsev, V. Sidorov, L. Shelimova, et al., Phys. Status Solidi A 74 (1982) 185–192.
[28] R. Bellissent, C. Bergman, R. Ceolin, J.-P. Gaspard, Phys. Rev. Lett. 59 (1987) 661.
[29] J.Y. Raty, V. Godlevsky, P. Ghosez, C. Bichara, J.-P. Gaspard, J.R. Chelikowsky, Phys. Rev. Lett. 85 (2000) 1950–1953, http://dx.doi.org/10.1103/PhysRevLett.85.1950.
[30] B. Aufray, A. Kara, S. Vizzini, H. Oughaddou, C. Léandri, B. Ealet, G. Le Lay, Appl. Phys. Lett. 96 (2010), http://dx.doi.org/10.1063/1.3419932, http://scitation.aip.org/content/aip/journal/apl/96/18/10.1063/1.3419932.
[31] P. De Padova, C. Quaresima, P. Perfetti, B. Olivieri, C. Leandri, B. Aufray, S. Vizzini, G. Le Lay, Nano Lett. 8 (2008) 271–275, http://dx.doi.org/10.1021/nl072591y, pMID:18092826.
[32] E. Sheka, L. Chernozatonskii, J. Exp. Theor. Phys. 110 (2010) 121–132.
[33] G. Barrera, J. Bruno, T. Barron, N. Allan, J. Phys. Condens. Matter 17 (2005) R217.
[34] M. Krbal, A.V. Kolobov, P. Fons, J. Tominaga, S. Elliott, J. Hegedus, A. Giussani, K. Perumal, R. Calarco, T. Matsunaga, et al., Phys. Rev. B 86 (2012) 045212.
[35] G. Zhao, Y. Wu, Phys. Rev. B 79 (2009) 184203.
[36] C. Otjacques, J.-Y. Raty, M.-V. Coulet, M. Johnson, H. Schober, C. Bichara, J.-P. Gaspard, Phys. Rev. Lett. 103 (2009) 245901.
[37] C. Otjacques, J.-Y. Raty, F. Hippert, H. Schober, M. Johnson, R. Céolin, J.-P. Gaspard, Phys. Rev. B 82 (2010) 054202.
[38] S.R. Ovshinsky, Phys. Rev. Lett. 21 (1968) 1450.

[39] V.L. Deringer, R. Dronskowski, M. Wuttig, Adv. Funct. Mater. 25 (40) (2015) 6343–6359, http://dx.doi.org/10.1002/adfm.201500826.
[40] J.Y. Raty, W. Zhang, J. Luckas, C. Chen, R. Mazzarello, C. Bichara, M. Wuttig, Nat. Commun. 6 (2015).
[41] P. Littlewood, J. Phys. C, Solid State Phys. 13 (1980) 4855.
[42] P. Littlewood, J. Phys. C, Solid State Phys. 13 (1980) 4875.